TIERS Information Technology Journal
Vol.3, No.1, Juni 2022, pp. 01~10
ISSN: 2723-4533 / E-ISSN: 2723-4541
DOI: 10.38043/tiers.v3i1.3604

Predictive Modeling Classification of Post-Flood and Abrasion Effects With Deep Learning Approach

Finki Dona Marleny[1], Mambang[2]
finkidona@umbjm.ac.id[1], mambang@unism.ac.id[2]
[1]Department of Informatic, University of Muhammadiyah Banjarmasin, South Kalimantan, Indonesia
[2] Department of Information Technology, Sari Mulia University, South Kalimantan, Indonesia

ABSTRACT

Floods and abrasion are the most common disasters in Indonesia. A lot of data is collected from post-flood and abrasion disasters. From the data released by BNPB, disaster data is directly based on the occurrence of disasters. From these data, we will test predictive modeling classification with a deep learning approach. Big data can be made through classification and predictive modeling. Our proposed model is a classification of predictive modeling of post-flood and abrasion data using the H2O deep learning approach. Deep learning H2O models can also be evaluated with specific model metrics, termination metrics, and performance charts. This approach is used to optimize the performance and accuracy of predictions during the modeling process using our dataset pool training. The big data to be processed will generate new knowledge for policies in decision-making. Big data performance modeled with Deep Learning H2O is used to predict the Survival attributes of post-flood and abrasion sample datasets. The best metric performance is obtained from the maxout activation function with a 200-200 unit layer that gets an accuracy of 93.49% with AUC: 0.808 +/- 0.022 (micro average: 0.808).

Keywords: Deep Learning; Flood; Abrasion; Classification; Predictive;

Article Info

Accepted : 30-05-2022
Revised : 01-05-2022
Published Online : 25-06-2022

Correspondence Author:

Finki Dona Marleny
University of Muhammadiyah Banjarmasin
South Kalimantan, Indonesia
Email: finkidona@umbjm.ac.id

1. INTRODUCTION

Disasters can occur directly and suddenly or case slowly[1]. Disasters that case can cause damage and fatalities[2]. Disasters have types and characteristics[3], [4]. Disaster characteristics can be classified and predicted according to the level of risk[5]. From the data released by the National Disaster Management Agency (BNPB) in Indonesia Floods are the most frequent disaster events in Indonesia the data can be views on the official BNPB website page. Post-flood impacts can cause a lot of damage[6]. The most common result of post-flood is damage to the facilities or residences of the population[7]–[10]. Seawater that exceeds normal limits can cause damage at sea and on land. If there is a tidal wave in the sea, it can cause a sweep of the seaside area or called abrasion[11]. Abrasion causes some areas eroded by seawater to disappear[12]. The loss of coastal suburbs due to abrasion due to tidal waves has an impact on damage to facilities, homes, and community businesses in the area. As the largest archipelago, Indonesia is vulnerable to floods and abrasion disasters[13]–[15]. Flooding and abrasion are generally triggered by high rainfall, given changes in rainfall patterns[16]. The data released directly by BNPB is based on disaster events that occurred in disaster-affected areas. Big data can be created to test Predictive Modeling of Post-Flood and Abrasion Effects. As a result of the disaster, many fatalities and damage were caused. Victims are categorized as dead, missing, injured, suffering, and displaced.

Damage data is categorized into two, namely houses with heavy damage, moderately damaged, lightly damaged, and submerged houses. and damaged facilities such as Education, Health, bridges, worship, and offices[14]. This post-flood and abrasion impact data can be analyzed to model to provide meaningful information to support flood and abrasion mitigation and management decisions[9], [18]. Post-flood and abrasion data have irregular patterns but it is likely that the data that appears often occurs.

In recent years, machine learning has been combined and applied in many flood-related dataset studies.[16], [18]–[20]. Machine learning uses computational algorithms to evaluate information and develop predictions with big data.[20]. This approach to using machine learning is deep learning which is very useful in a rare area of data.[19].

From Indonesia's geoportal disaster data there is no model for analyzing big data due to post-flood and abrasion. Data that is available in real-time if not reprocessed then only limited to information. The data presented if only information then cannot help in decision making. If the performance of the data is not validated then the data is not known the performance of the data and the performance data. Deep learning is more often used for image analysis, can post-flood and abrasion data be used to measure predictive modeling classification modeling performance with H2O deep learning.

The analysis uses deep learning modeling for predictive modeling classification[18], [21], [22]. The approach used for data due to post-flood and abrasion is with H2O deep learning to perform classification[19], [20] . Big data is trained using role sets from the Predictive Modeling Classification process[18]. Many different parameters can be given to H2O deep learning methods. The performance of learning model results data is divided into training and testing through cross-validation. Cross-validation makes it possible to estimate model performance more accurately and reliably[24]. The data is used in real-time following the occurrence of flood disasters and abrasion from geoportal data disaster data. The data to be tested into the H2O deep learning model goes through the modeling and data testing training procedures. During further model creation, explore the various core components and functions of H2O[25].

Deep learning H2O models can also be evaluated with specific model metrics, termination metrics, and performance charts[26]. Deep learning H2O models can also be evaluated with specific model metrics, termination metrics, and performance charts.[27].

Deep learning can identify irregular patterns[28]. Post-flood and abrasion data have irregular patterns because data is obtained from direct events per day. But it could be that data cannot be collected per day because there is no disaster. Models for analyzing big data due to post-flood and abrasion with deep learning H2O are used for big data efficiency[29], [30]. Data available in real-time retrieved for reprocessing is not just limited to information. The big data to be processed will generate new knowledge for policies in decision making. Big data performance modeled with Deep Learning H2O is used to predict the Survival attributes of post-flood and abrasion sample datasets.

This research is important because it can provide an overview of the classification of predictive modeling of post-flood data. The data tested using this deep learning method becomes new knowledge in machine learning. The model we propose is a predictive modeling classification of post-flood and abrasion data using the H2O deep learning approach. This approach is used to optimize prediction performance and accuracy during the modeling process using our dataset training. We compared the proposed new deep learning outcomes with other computational benchmark models.

2. RESEARCH METHOD

The methodological steps are as follows in figure 1. In conducting a deep learning approach to Predictive Modeling Classification the first step using data that has been cleaned up. Then the data is per the role set. The next step is the stage of cross-validation performance of a learning model resultant data is split into training and testing. Furthermore, in the training process using H2O Deep Learning operators profit apply the model. In the testing process, a trained model has been applied to labeled data. The final stage is the result of the performance binominal classification, namely the accuracy of the model compute model assessed.

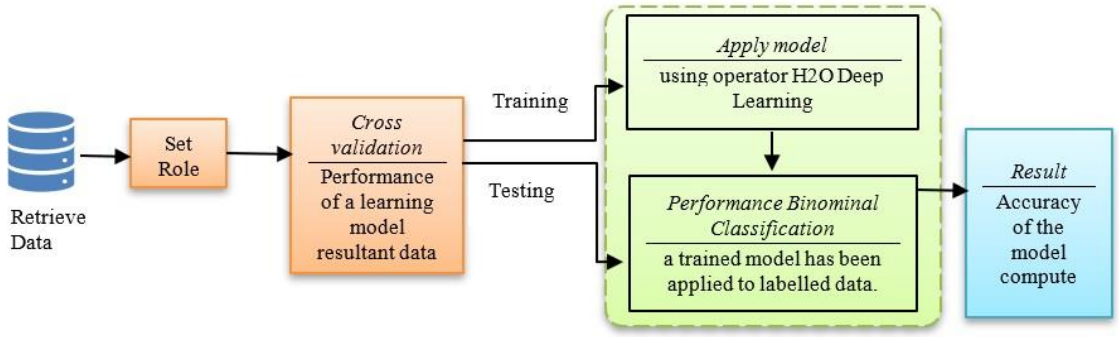

Figure 1. Process flow diagram of the proposed work

2.1. Data Collection

The data collection is data from the official website of the National Disaster Management Agency(BNPB), geoportal Indonesian disaster data on the https://gis.bnpb.go.id/ page. The data taken as test data is data from 2018 to 2021 of the types of flood and abrasion disaster events. The total duration of 1460 days of data is an example set of 5423 examples. Attribute meta data information used can be seen in the table below.

Table 1. Attribute meta data information

Attribute	Type data
Date of event	Date
Types of disaster events	Binominal
Regency	Polyniminal
Province	Integer
Die	Integer
Disappear	Integer
Injured	Integer
Broken House	Integer
Submerged House	Integer

2.2. Set Role

The set role attribute role describes how other Operators handle Attributes in the data. Other Roles are classified as special. An ExampleSet can have many special Attributes, but each custom role can only appear once. If a special role is assigned to more than one Attribute, all roles will be changed to regular except for the last Attribute. Role Sets are used to change the roles of one or more Attributes. The parameter used is the name of the attribute whose role must be changed then the range target_peran. The target role of the selected Attribute is the new role assigned to it[25].

2.3. Overview Deep Learning Algorithm

Deep learning is a subfield of machine learning that is part of artificial intelligence.[31]. Deep learning consists of several artificial neural networks that are interconnected[26], [30]. Deep Learning classification or regression model delivered from the output port[30], [31]. This regression classification or model can be applied to invisible data sets for label attribute prediction[22]. In its application, deep learning can identify irregular patterns or not follow the predicted behavior. Anomalies can be interpreted as unnatural behavior or patterns and can be a sign of errors in the system.[22]. In this case, deep learning can be relied on to measure the performance of irregular data patterns.[27], [32]. Model Deep Learning H2O can be used to perform guided classification and regression[22].

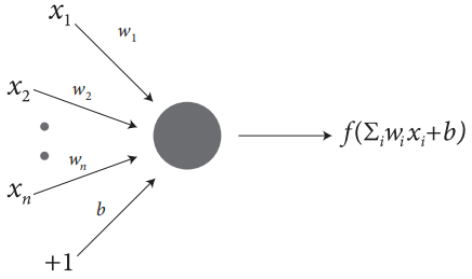

Figure 2. The basic unit in the model

Tanh Activation functions. In the model, the weighted combination of input signals is aggregated, and then an output signal $f(\alpha)$ is transmitted by the connected neuron. The function f represents the nonlinear activation function used throughout the network, and the bias b accounts for the neuron's activation threshold[26].

$$\alpha = \sum_{i=1}^{n} w_i x_i + b \quad (1)$$

Deep learning is based on a multi-layer feed-forward artificial neural network consisting of a layer consisting of many layers of interconnected neuronal units, starting with the input layer to match the feature space, then continuing with several nonlinear layers, and ending with a linear regression or classification layer to fit the output space[20]. The input and output of the model unit follow the basic logic of a single neuron described above. Bias units are included in each non-output layer of the network. The weight that connects neurons and biases with other neurons fully determines the output of the entire network, and learning occurs when these weights are adjusted to minimize errors in labeled training data. More specifically, for each example of j training, the goal is to minimize the function of loss[33].

2.4. Activation Function

Activation function provides output based on the input signal. The network of deep learning algorithm architectures can contain a large number of hidden layers. These layers consist of neurons with activation functions. There are several activation functions used such as ReLU, Maxout, and Tanh functions[27], [30].

The Rectified linear activation function or ReLU for short is a linear function of pieces that will output inputs directly if positive, otherwise, will produce zero. Rectified Linear implements the following functions:

$$f(\alpha) = \max(0, \alpha) \quad (2)$$

The Maxout activation function can be interpreted as creating a linear approximation of pieces to an arbitrary convex function. Maxout unit implements the following functions:

$$f(\cdot) = \max(w_i x_i + b), \text{rescale if max } f(\cdot) \geq 1 \quad (3)$$

The activation function of hyperbolic tangents is also referred to simply as Tanh. This function takes any real value as input and output values in the range of -1 to 1. The larger the input, the closer the output value will be to 1.0, while the smaller the input, the closer the output will be to -1.0. Tanh implements the following functions:

$$f(\alpha) = \frac{e^{\alpha} - e^{-\alpha}}{e^{\alpha} + e^{-\alpha}} \quad (4)$$

2.5. Loss Function

This experiment uses the loss function cross entropy which is a typical use classification. The following choices for the loss function L(W, B | j). The system default enforces typical use rules based on whether regression or classification is being performed. Note here that t (j) and o(j) are the predicted (target) output and actual output, respectively, for training example j; further, let y denote the output units and 0 the output layer[34]–[36].

$$\mathrm{L(W, B \mid j)} = -\sum_{y \epsilon 0} (\ln(0_y^{(j)}) . t_y^{(j)} + ln(1 - 0_y^{(j)}) . (1 - t_y^{(j)})) \quad (5)$$

2.6. Bernoulli Distribution

Discrete probability distributions are used in machine learning, especially in modeling binary and multi-class classification issues, but also in evaluating performance for binary classification models, such as trust interval calculations, and in modeling the distribution of words in a text[37], [38]. The Bernoulli distribution uses binary random variables. Distribution function for training data[39]. Some further tuning functions can be achieved through expert parameters[40]. Bernoulli distribution can be used for binominal atau 2-class polynominal labels.

$$X \sim \text{Bernoulli}(p) \quad (6)$$

The cumulative distribution function is:

$$F(x) = \begin{cases} 0 \; x < 0 \\ 1 - p \; 0 \leq x < 1, \\ 1 \; x \geq 1 \end{cases} \quad (7)$$

3. RESULTS AND DISCUSSION

The resulting process uses standard rules of modeling parameters from the H2O deep learning approach. in the Performance of a learning model of the data training process compares the performance of the activation functions of ReLU, Maxout, and Tanh. Hiden layer units are trained to start from 50, 100, and 200 hidden layers. A small part of the input of each hidden layer will be omitted from the training to improve generalizations. Epoch 10.0, for train sample per-interation, starting from -2. Epsilon 1.0e-8, similar to learning rate during initial training and momentum at a later stage that allows forward. Almost the same as momentum and relates to memory in weight intermingling, the typical value of rho is between 0.99 and 0.999. The L1 has a value of 1.0E-5 regulatory methods that can limit the absolute value of the weight and has the net effect of setting to zero the model to reduce complexity and avoid overfitting. L2 is a regulatory method that limits the amount of squared weight. This method introduces bias into parameter estimation. Max w2 is the maximum amount of weight entered squared into a neuron that is given a value of 10.0. The loss function serves to be minimized by the model, in this training the model consists of independent hypotheses so we use cross entropy only. The distribution of functions for training data uses Bernoulli because the data has a 2 class label. The metric results reported on the binomial complete training model frame metric type. It can be seen in the results of table 1 that the unit layer 200-200 has better performance.

Table 2. Reported on full training frame

Activation	Layer Units	MSE	RMSE	R^2	AUC	Pr_auc	Log Loss	Mean per class error	Default threshold
ReLU	200	0.029749	0.172481	0.197128	0.862796	0.358086	0.134157	0.286818	0.220939
Tanh	200	0.031477	0.177419	0.150498	0.903135	0.296896	0.118166	0.244644	0.096136
Maxout	200	0.030279	0.174009	0.182839	0.919249	0.392624	0.118398	0.241480	0.065915
ReLU	100	0.029385	0.171422	0.206953	0.917704	0.369568	0.109243	0.230094	0.137782
Tanh	100	0.031036	0.176172	0.162401	0.913704	0.309998	0.112730	0.258706	0.173461
Maxout	100	0.029322	0.171239	0.208651	0.926698	0.363578	0.105916	0.255925	0.155138
ReLU	50	0.030575	0.174858	0.174849	0.857628	0.328813	0.136700	0.272954	0.130298
Tanh	50	0.036628	0.191385	0.011488	0.743031	0.161231	0.165262	0.354233	0.031157
Maxout	50	0.030656	0.175091	0.172646	0.898218	0.331372	0.120846	0.286733	0.144114

The status of the Neuron Layer can be seen in the table below. The results of predicting types of disasters, 2-class classification, the results in these tables are the best results from the activation function in the training. We tested hidden layer layers ranging from 50, 100, and 200. Bernoulli distribution is used for discrete probability distributions where Bernoulli's random variable can only have 0 or 1 as a result. Bernoulli's distribution matches the conditions of the data in the training. CrossEntropy loss is used to optimize classification models. Cross-Entropy understanding on understanding Softmax activation function. Softmax converts logs into probabilities aimed at making the model output as close to the desired output as possible. Here are the results of the status of the neuron layer of units 200-200 with reLU, tanh, and maxout activation functions that have better performance and performance than other layer units

Table 3. Status of Neuron Layers Relu activation function

Layer	Units	Lift Cumulative	Mean Rate	Rate RMS	Weight	Weight RMS	Bias	Bias RMS
1	519	Input						
2	200	Relu	0.158634	0.273293	0.001037	0.054106	-0.061495	0.106414
3	200	Relu	0.224868	0.309316	-0.002743	0.059619	0.730693	0.341669
4	2	Softmax	0.068742	0.212369	-0.007770	0.205507	0.001542	0.000883

Table 4. Status of Neuron Layers Tanh activation function

Layer	Units	Lift Cumulative	Mean Rate	Rate RMS	Weight	Weight RMS	Bias	Bias RMS
1	519	Input						
2	200	Tanh	0.111265	0.185469	0.000142	0.054190	0.004304	0.037411
3	200	Tanh	0.472069	0.437979	-0.000042	0.048406	0.001674	0.034231
4	2	Softmax	0.271041	0.271041	-0.015211	0.180501	-0.000168	0.110938

Table 5. Status of Neuron Layers Maxout activation function

Layer	Units	Lift Cumulative	Mean Rate	Rate RMS	Weight	Weight RMS	Bias	Bias RMS
1	519	Input						
2	200	Maxout	0.215083	0.350278	0.001268	0.054008	0.029617	0.120012
3	200	Maxout	0.263552	0.313712	-0.005478	0.058934	0.898479	0.150922
4	2	Softmax	0.002412	0.001650	-0.017639	0.202034	-0.000353	0.000193

From the results of the training scoring history with layers, 200-200 has a longer duration and training speed than other unit layers. The following table is the result of a scoring history of the best training performance.

Table 6. History Scoring with ReLU activation function

Duration	Training Speed	Epochs	Iterations	Samples Training	RMSE Training	LogLoss	Training Classifications error
5.122 sec	1333 obs/sec	1.00000	1	5423	0.19353	0.18116	0.06085
14.906 sec	1641 obs/sec	4.00000	4	21692	0.18155	0.13834	0.06196
23.793 sec	1773 obs/sec	7.00000	7	37961	0.17829	0.14370	0.05680
28.461 sec	2122 obs/sec	10.00000	10	54230	0.17248	0.13416	0.04370

Table 7. History Scoring with Tanh activation function

Duration	Training Speed	Epochs	Iterations	Samples Training	RMSE Training	LogLoss	Training Classifications error
2.121 sec	2381 obs/sec	0.65554	1	3555	0.18855	0.14689	0.07929
7.609 sec	2206 obs/sec	2.59174	4	14055	0.18067	0.12866	0.07026
13.985 sec	2057 obs/sec	4.54507	7	24648	0.17742	0.11817	0.06417
21.680 sec	2019 obs/sec	7.12945	11	38663	0.17893	0.12072	0.05956
27.614 sec	2006 obs/sec	9.05292	14	49094	0.20371	0.15058	0.04739
31.482 sec	2013 obs/sec	10.34354	16	56093	0.18842	0.14681	0.05255
32.019 sec	2011 obs/sec	10.34354	16	56093	0.17742	0.11817	0.06417

Table 8. History Scoring with Maxout activation function

Duration	Training Speed	Epochs	Iterations	Samples Training	RMSE Training	LogLoss	Training Classifications error
2.248 sec	1117 obs/sec	0.18274	1	991	0.19610	0.23948	0.13351
16.059 sec	1122 obs/sec	2.69039	15	14590	0.18748	0.16351	0.05053
33.489 sec	1230 obs/sec	6.51079	36	35308	0.17401	0.11840	0.05809
50.688 sec	1223 obs/sec	10.08427	56	54687	0.17484	0.12111	0.04204
52.591 sec	1219 obs/sec	10.08427	56	54687	0.17401	0.11840	0.05809

The ROC curve is a graph that shows the performance of the classification model at all classification thresholds. This curve plots two parameters of the true positive level and the false positive level. While the AUC serves to measure the entire two-dimensional area under the entire ROC curve. The following is a look at the results of the AUC from the training that has been tested.

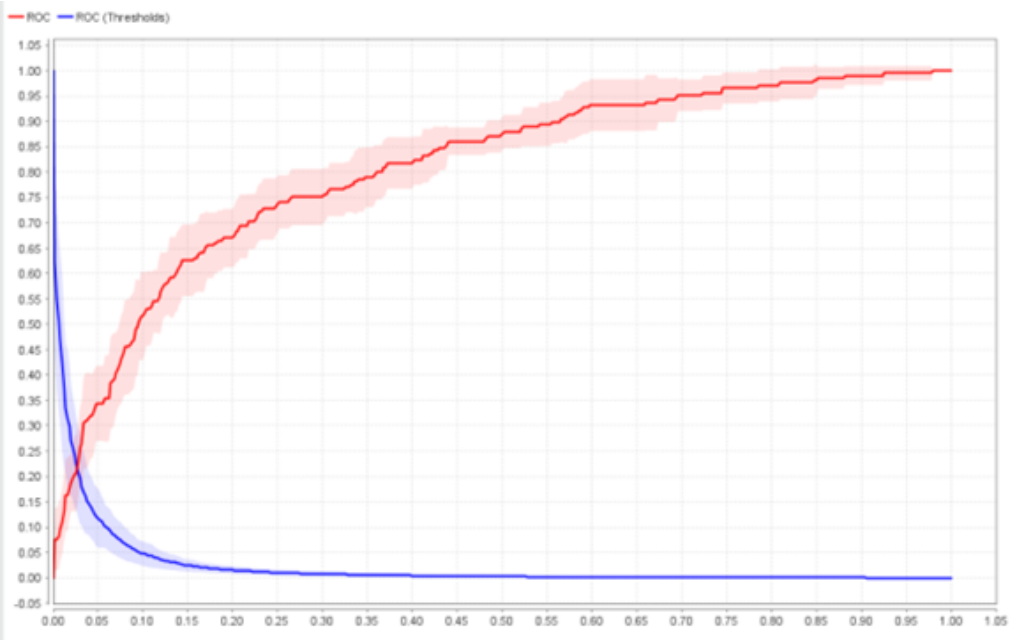

Figure 3. AUC: 0.808 +/- 0.022 (micro average: 0.808)

The image above is the best AUC result of each layer unit trained. Figure 3 describes the best performance and performance of layer units 200-200 AUC charts.

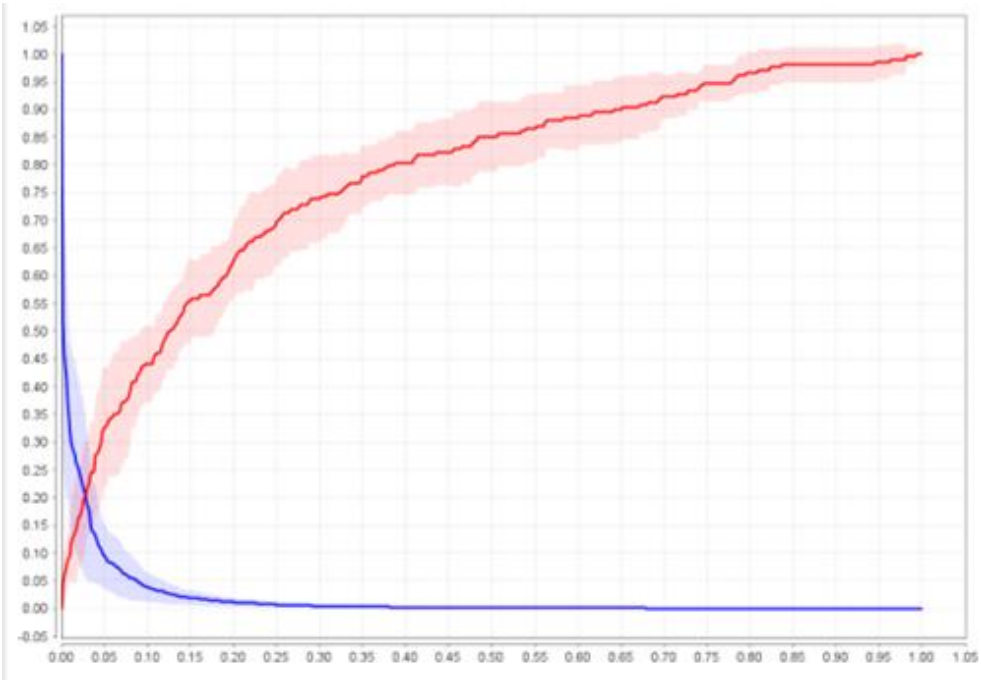

Figure 4. AUC: 0.779 +/- 0.040 (micro average: 0.779)

Figure 4 describes the performance and performance of the use of Activation ReLU with layer units 100-100.

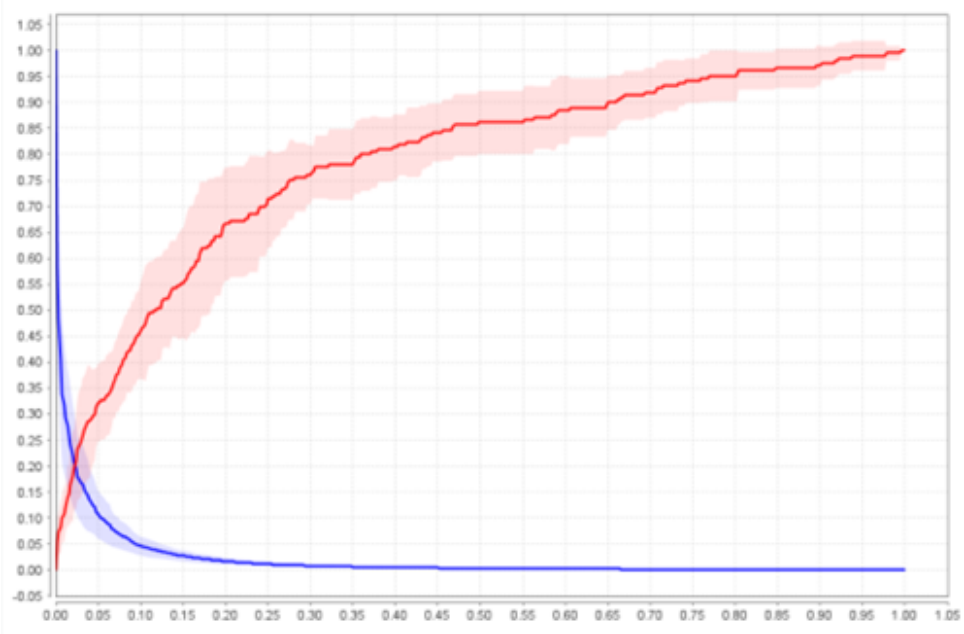

Figure 5. AUC: 0.786 +/- 0.044 (micro average: 0.786)

Last in figure (c) is layer units 50-50 AUC charts with maxout activation function.

4. CONCLUSION

The resulting model is the classification of predictive modeling of post-flood and abrasion data using the H2O deep learning approach testing training and testing data with different activation functions and varying unit layers get the result that by using the maxout activation function get an accuracy of 93.49% with AUC: 0.808 +/- 0.022 (micro average: 0.808). Unit layers tested 200-200 with large layers have the disadvantage of Assessment History with a longer duration compared to using unit layers 50-50. This approach is used to optimize the performance and accuracy of predictions during the modeling process using our dataset pool training. We compared the proposed new deep learning results with other computational benchmark models of the activation function and obtained no better performance than maxout and ReLU activation functions. Layer 50-50 obtained good performance results with the use of the maxout activation function. Likewise, layer 100-100 gets good performance by using the ReLU activation function. In the case of our data, the use of maxout activation has better performance and performance compared to other model uses. The advice for other researchers is to be able to add more data so that when cross-validating it can be more optimal and have better performance and performance in the future.

REFERENCES

[1] T. Mondal, N. Boral, I. Bhattacharya, J. Das, and P. Pramanik, *Distribution of deficient resources in disaster response situation using particle swarm optimization*, vol. 41. Elsevier Ltd, 2019.

[2] D. Wu and Y. Cui, "Disaster early warning and damage assessment analysis using social media data and geo-location information," *Decis. Support Syst.*, vol. 111, no. April, pp. 48–59, 2018, doi: 10.1016/j.dss.2018.04.005.

[3] J. Son, H. K. Lee, S. Jin, and J. Lee, "Content features of tweets for effective communication during disasters: A media synchronicity theory perspective," *Int. J. Inf. Manage.*, vol. 45, no. October 2018, pp. 56–68, 2019, doi: 10.1016/j.ijinfomgt.2018.10.012.

[4] K. Muhammad, J. Ahmad, and S. W. Baik, "Early fire detection using convolutional neural networks during surveillance for effective disaster management," *Neurocomputing*, vol. 288, pp. 1–27, May 2018, doi: 10.1016/j.neucom.2017.04.083.

[5] I. A. Rana, M. Asim, A. B. Aslam, and A. Jamshed, "Disaster management cycle and its application for flood risk reduction in urban areas of Pakistan," *Urban Clim.*, vol. 38, no. February, pp. 1–12, Jul. 2021, doi: 10.1016/j.uclim.2021.100893.

[6] X. Guan, Y. Zang, Y. Meng, Y. Liu, H. Lv, and D. Yan, "Study on spatiotemporal distribution characteristics of flood and drought disaster impacts on agriculture in China," *Int. J. Disaster Risk Reduct.*, vol. 64, no. August, pp. 1–13, 2021, doi: 10.1016/j.ijdrr.2021.102504.

[7] E. Yulianto, D. A. Yusanta, P. Utari, and I. Agung, "International Journal of Disaster Risk Reduction Community adaptation and action during the emergency response phase : Case study of natural disasters in Palu , Indonesia,"

Int. J. Disaster Risk Reduct., vol. 65, no. June 2020, pp. 2–11, 2021, doi: 10.1016/j.ijdrr.2021.102557.

[8] M. K. Htein, S. Lim, and T. N. Zaw, "The evolution of collaborative networks towards more polycentric disaster responses between the 2015 and 2016 Myanmar floods," *Int. J. Disaster Risk Reduct.*, vol. 31, pp. 964–982, 2018, doi: 10.1016/j.ijdrr.2018.08.003.

[9] L. Tan and D. M. Schultz, "Damage classification and recovery analysis of the Chongqing, China, floods of August 2020 based on social-media data," *J. Clean. Prod.*, vol. 313, no. February, pp. 2–12, 2021, doi: 10.1016/j.jclepro.2021.127882.

[10] A. Kawasaki, N. Ichihara, Y. Ochii, R. A. Acierto, A. Kodaka, and W. W. Zin, "Disaster response and river infrastructure management during the 2015 Myanmar floods: A case in the Bago River Basin," *Int. J. Disaster Risk Reduct.*, vol. 24, pp. 151–159, 2017, doi: 10.1016/j.ijdrr.2017.06.004.

[11] Q. Qin, Q. Meng, H. Yang, and W. Wu, "Study of the anti-abrasion performance and mechanism of coral reef sand concrete," *Constr. Build. Mater.*, vol. 291, p. 123263, 2021, doi: 10.1016/j.conbuildmat.2021.123263.

[12] Y. A. Mehanna and C. R. Crick, "Image analysis methodology for a quantitative evaluation of coating abrasion resistance," *Appl. Mater. Today*, vol. 25, p. 101203, 2021, doi: 10.1016/j.apmt.2021.101203.

[13] N. A. Pinontoan and U. Wahid, "Analisis Framing Pemberitaan Banjir Jakarta Januari 2020 Di Harian Kompas.Com Dan Jawapos.Com," *Komuniti J. Komun. dan Teknol. Inf.*, vol. 12, no. 1, pp. 11–24, 2020, doi: 10.23917/komuniti.v12i1.9928.

[14] R. K. Chandra and R. D. Supriharjo, "Mitigasi Bencana Banjir Rob di Jakarta Utara," *J. Tek. Pomits*, vol. 2, no. 1, pp. 25–30, 2013.

[15] A. Maulana, B. Kusumasari, and S. R. Giyarsih, "Komunikasi Bencana di Twitter: Studi Kasus Bencana Banjir Perkotaan di Daerah Khusus Ibukota (DKI) Jakarta`," *J. Kawistara*, vol. 11, no. 2, p. 129, 2021, doi: 10.22146/kawistara.v11i2.58123.

[16] X. Lei *et al.*, "Urban flood modeling using deep-learning approaches in Seoul, South Korea," *J. Hydrol.*, vol. 601, p. 126684, 2021, doi: 10.1016/j.jhydrol.2021.126684.

[17] A. Damayanti, F. Arifianto, and T. L. Indra, "Development Area for Floating Solar Panel and Dam in The Former Mine Hole (Void) Samarinda City, East Kalimantan Province," *Int. J. Adv. Sci. Eng. Inf. Technol.*, vol. 11, no. 5, pp. 1713–1720, 2021, doi: 10.18517/ijaseit.11.5.14097.

[18] M. Panahi *et al.*, "Deep learning neural networks for spatially explicit prediction of flash flood probability," *Geosci. Front.*, vol. 12, no. 3, p. 101076, 2021, doi: 10.1016/j.gsf.2020.09.007.

[19] H. Shahabi *et al.*, "Flash flood susceptibility mapping using a novel deep learning model based on deep belief network, back propagation and genetic algorithm," *Geosci. Front.*, vol. 12, no. 3, p. 101100, 2021, doi: 10.1016/j.gsf.2020.10.007.

[20] H. Hosseiny, "A deep learning model for predicting river flood depth and extent," *Environ. Model. Softw.*, vol. 145, p. 105186, 2021, doi: 10.1016/j.envsoft.2021.105186.

[21] C. Wang *et al.*, "Deep learning for predicting subtype classification and survival of lung adenocarcinoma on computed tomography," *Transl. Oncol.*, vol. 14, no. 8, p. 101141, 2021, doi: 10.1016/j.tranon.2021.101141.

[22] D. Passos and P. Mishra, "A tutorial on automatic hyperparameter tuning of deep spectral modelling for regression and classification tasks," *Chemom. Intell. Lab. Syst.*, vol. 223, no. October 2021, 2022, doi: 10.1016/j.chemolab.2022.104520.

[23] Y. Qian *et al.*, "Classification of rice seed variety using point cloud data combined with deep learning," vol. 14, no. 5, pp. 206–212, 2021, doi: 10.25165/j.ijabe.20211405.5902.

[24] S. De Bruin, D. J. Brus, G. B. M. Heuvelink, T. Van Ebbenhorst, and A. M. J. Wadoux, "Ecological Informatics Dealing with clustered samples for assessing map accuracy by," *Ecol. Inform.*, vol. 69, no. May, p. 101665, 2022, doi: 10.1016/j.ecoinf.2022.101665.

[25] S. K. Sundhara, G. Krishna, N. Bhalaji, and S. Chithra, "BCI cinematics – A pre-release analyser for movies using H 2 O deep learning platform," *Comput. Electr. Eng.*, vol. 74, pp. 547–556, 2019, doi: 10.1016/j.compeleceng.2018.03.015.

[26] W. Zhu *et al.*, "Phase formation prediction of high-entropy alloys: a deep learning study," *J. Mater. Res. Technol.*, vol. 18, pp. 800–809, 2022, doi: 10.1016/j.jmrt.2022.01.172.

[27] S. Y. Lee, S. Byeon, H. S. Kim, H. Jin, and S. Lee, "Deep learning-based phase prediction of high-entropy alloys: Optimization, generation, and explanation," *Mater. Des.*, vol. 197, p. 109260, 2021, doi: 10.1016/j.matdes.2020.109260.

[28] L. Talavera-Martínez, P. Bibiloni, A. Giacaman, R. Taberner, L. J. D. P. Hernando, and M. González-Hidalgo, "A novel approach for skin lesion symmetry classification with a deep learning model," *Comput. Biol. Med.*, vol. 145, no. September 2021, p. 105450, 2022, doi: 10.1016/j.compbiomed.2022.105450.

[29] B. Harangi, A. Baran, and A. Hajdu, "Assisted deep learning framework for multi-class skin lesion classification considering a binary classification support," *Biomed. Signal Process. Control*, vol. 62, p. 102041, 2020, doi: 10.1016/j.bspc.2020.102041.

[30] M. Čokina, V. Maslej-Krešňáková, P. Butka, and Parimucha, "Automatic classification of eclipsing binary stars using deep learning methods," *Astron. Comput.*, vol. 36, p. 100488, 2021, doi: 10.1016/j.ascom.2021.100488.

[31] M. Aljabri *et al.*, "Canine impaction classification from panoramic dental radiographic images using deep learning models," *Informatics Med. Unlocked*, vol. 30, no. December 2021, p. 100918, 2022, doi: 10.1016/j.imu.2022.100918.

[32] L. Wang, J. Wang, Z. Liu, J. Zhu, and F. Qin, "Evaluation of a deep-learning model for multispectral remote sensing of land use and crop classification," *Crop J.*, no. xxxx, 2022, doi: 10.1016/j.cj.2022.01.009.

[33] F. Cui, S. Li, Z. Zhang, M. Sui, C. Cao, and A. E. Hesham, "DeepMC-iNABP : Deep learning for multiclass

identification and classification of nucleic acid-binding proteins," *Comput. Struct. Biotechnol. J.*, vol. 20, pp. 2020–2028, 2022, doi: 10.1016/j.csbj.2022.04.029.

[34] S. Paul, B. Jhamb, D. Mishra, and M. S. Kumar, "Edge loss functions for deep-learning depth-map," *Mach. Learn. with Appl.*, vol. 7, no. June 2021, p. 100218, 2022, doi: 10.1016/j.mlwa.2021.100218.

[35] Y. Li, R. Qian, and K. Li, "Inter-patient arrhythmia classification with improved deep residual convolutional neural network," *Comput. Methods Programs Biomed.*, vol. 214, 2022, doi: 10.1016/j.cmpb.2021.106582.

[36] F. Olsen, C. Schillaci, M. Ibrahim, and A. Lipani, "Borough-level COVID-19 forecasting in London using deep learning techniques and a novel MSE-Moran's I loss function," *Results Phys.*, vol. 35, no. January 2021, p. 105374, 2022, doi: 10.1016/j.rinp.2022.105374.

[37] Z. Huang *et al.*, "A seven-parameter Bernoulli-Gamma-Gaussian model to calibrate subseasonal to seasonal," *J. Hydrol.*, p. 127896, 2022, doi: 10.1016/j.jhydrol.2022.127896.

[38] R. Eberle and M. Oberguggenberger, "A new method for estimating the bending stiffness curve of non-uniform Euler-Bernoulli beams using static deflection data," *Appl. Math. Model.*, vol. 105, pp. 514–533, 2022, doi: 10.1016/j.apm.2021.12.042.

[39] R. Li, B. J. Reich, and H. D. Bondell, "Deep distribution regression," *Comput. Stat. Data Anal.*, vol. 159, p. 107203, 2021, doi: 10.1016/j.csda.2021.107203.

[40] R. Zheng, S. Zhang, L. Liu, Y. Luo, and M. Sun, "Uncertainty in Bayesian deep label distribution learning," *Appl. Soft Comput.*, vol. 101, p. 107046, 2021, doi: 10.1016/j.asoc.2020.107046.